Accurate carrier-type determination of nonhomogenously doped diamond

N. Yom-Tov,[1,2] C. Saguy,[2] A. Bolker,[2] R. Kalish,[2] and Y. E. Yaish[1,a)]
[1]*Department of Electrical Engineering, Technion, Haifa 32000, Israel*
[2]*Department of Physics, Solid State Institute, Technion, Haifa 32000, Israel*

(Received 14 April 2010; accepted 14 June 2010; published online 26 August 2010)

Electrical properties of B-doped homoepitaxialy grown diamond are characterized with and without mesa structures by Hall effect measurements as function of temperature in the as-grown state and following oxygen reactive ion etching (RIE). The extracted carrier type, concentration, and mobility are found to depend on the measurement contact configuration. For measurements performed without mesa major differences, even in carrier type, are found following the RIE treatment, however no changes what so ever are observed when measuring with a mesa structure. Finite element simulation confirms that carrier concentration or/and mobility inhomogeneities in the regions surrounding the contacts in Hall effect measurements using the Van der Pauw configuration can result in wrong assignments of carrier type, concentration and mobility. © *2010 American Institute of Physics*. [doi:10.1063/1.3463395]

I. INTRODUCTION

Among the many outstanding properties of diamond are its extremely high thermal conductivity and its high electric breakdown field. These make diamond a material of choice for electronic devices of unique properties.[1,2] To exploit these, however, it is of great importance to turn diamond conductive by appropriated doping and to be able to accurately determine its electrical properties (carrier type, concentration, and mobility). Whereas p-type doping of diamond is well under control, using B as the dopant, n-type doping with a shallow enough donor level, is problematic and is still the subject of intensive research with no clear conclusions as yet.[3] Some of the difficulties are related to the lack of suitable elemental dopants (P and N being too deep donors in diamond) and to problems related to the evaluation of the electrical properties of the doped regions. The latter depend on the availability of reproducible homogeneous intrinsic large area of high quality diamond. Furthermore, the presence of millimeter size growth sectors that often exist in single crystal diamond that serve as substrates for homoepitaxial over growth yield doping inhomogeneity in the overgrown B doped layer.[4–6] In addition, the extreme chemical and physical properties of diamond hamper application of common, dry and wet, clean room methods to realize localized submillimeter size structures in diamond to enable the application of accurate electrical measurements.

Here we describe ways of realizing submillimeter size mesa structures in diamond and present reliable results on the electrical properties of differently treated diamond samples. We show that the results of Hall measurements in Van der Pauw (VdP) configuration using four point contacts can yield substantially different results, including carrier type, as compared to those obtained from restricted area measurements as possible when employing mesa geometries. We present finite element simulations to explain these results. Finally, we discuss the relevance of these findings to the p-to n-type conversion reported for B doped diamond exposed to hydrogen plasma.[7]

II. EXPERIMENTAL

Type Ib ⟨100⟩ single crystal diamonds, $3\times3\times1$ mm^3, were homoepitaxially over-grown with a thin (~0.2 μm) undoped diamond layer followed by a 1 μm thick homoepi B doped layer.[8] Due to the thickness of the side facets of the substrates used, rather substantial diamond growth on the sample sides has also occurred. SIMS (secondary ion mass spectrometry) was used to obtain accurate layer thicknesses and B concentrations on both top (B^T) and side facets (B^S) of the samples. The boron concentrations on the side facets were found to be much higher than those on the top ($B^S \approx 10\times B^T$). The carrier type, concentration, and mobility were measured, as function of temperature ($80\ K<T<900\ K$), using Hall measurements in the VdP configuration with four contacts placed (i) on the top layer of the sample, and (ii) on mesa structures placed at selected locations on the top of the samples. Configurations (i) and (ii) are sketched in the insets of Figs. 1 and 2, respectively. The sample shape in (i) was square of $3\times3\times1$ mm^3 where the distance between two opposite contacts was 1.7 mm (inset of Fig. 1). Ti/Au contacts of 200×200 μm^2 were deposited 650 μm from the edges of the sample and annealed in nitrogen atmosphere for 30 min at 400 °C. For (ii), mesa structure of circular shape of 2.6 mm in diameter was produced (inset of Fig. 2) as follows:[9] (a) definition of mesa using photolithography, (b) deposition of 150 nm of NiCr mask that serves as stop layer for O_2 reactive ion etching (RIE), (c) O_2 RIE for 2 h for mesa fabrication and (d) removal of the NiCr mask. (e) After mesa definition, an additional lithography step was performed for contact definition. (f) Ti/Au contacts were deposited on the edges of the structured mesa. The mesa height was ~1.3 μm, deep enough to ensure electrical decoupling between the mesa and the side facets. After mesa definition a second RIE treatment was

a)Electronic mail: yuvaly@ee.technion.ac.il.

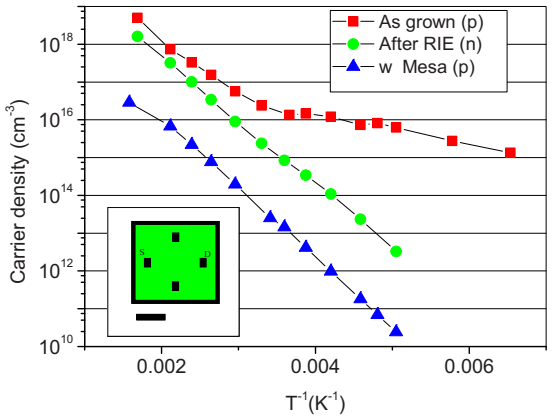

FIG. 1. (Color online) Carrier concentration vs T^{-1} for boron doped diamond. As grown sample 1 (square, p-type), exposed to O_2 RIE (circle, n-type), and after mesa definition (triangular, p-type). Inset: sample shape and dimension before mesa definition. Black squares are metallic contacts. Scale bar is 1 mm.

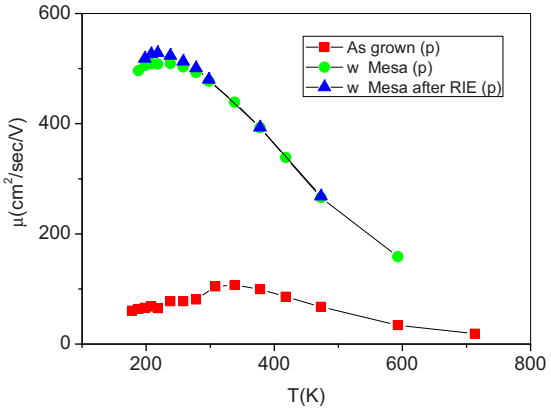

FIG. 3. (Color online) Mobility vs T for boron doped diamond. As grown sample 2 (square, p-type), after mesa definition (circle, p-type), and exposed to O_2 RIE (triangular, p-type).

done with the same conditions but for a shorter time (20 min) on the whole sample, and as a consequence the thickness of the boron doped top layer was reduced to 0.75 μm. Hall effect measurements as a function of temperature (80 K $<T<$ 900 K) and magnetic field of 0.8 T were carried out on samples with and without mesa structures.

III. RESULTS AND DISCUSSION

Figure 1 depicts the measured carrier concentrations before (squares) and after exposing sample 1 to 20 min oxygen plasma RIE (spheres) in configuration (i) (no mesa). The as-grown B doped diamond shows, as expected, p-type conductivity. Two activations energies are obtained: at high temperatures E_a=0.33 eV, whereas at low temperatures, E_a =0.1 eV. This behavior is characteristic of a highly doped B-doped sample with two conductivity regimes.[10] Thermally activated conduction dominates at higher temperatures while hopping conductivity occurs at lower temperatures. The carrier density at 500 °C is found to be $p=5\times10^{18}$ cm^{-3} which *exceeds the B concentration measured by SIMS* for the top of the sample ($B^T=2\times10^{18}$ cm^{-3}). Both the carrier concentration versus 1/T and the boron SIMS profiles measured on the as-grown sample suggest that the low activation energy at low temperatures (Fig. 1) is mainly due to the contribution of the side facets and not that of the top layer. After O_2 RIE the *conductivity turned from p- to n-type and the total conductance decreased by a factor of* ~5. Nevertheless, the activation energy remained the same as for a p-type diamond (E_a =0.33 eV) for the entire temperature range.

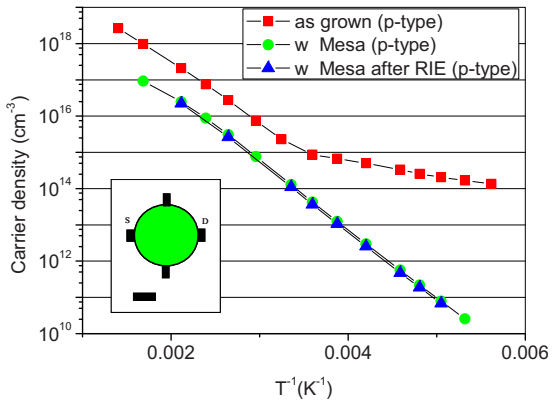

FIG. 2. (Color online) Carrier concentration vs T^{-1} for boron doped diamond. As grown sample 2 (square, p-type), after mesa definition (circle, p-type), and exposed to O_2 RIE (triangular, p-type). Inset: sample shape and dimension after mesa definition. Black squares are metallic contacts. Scale bar is 1 mm.

Figure 1 also shows (triangles) the carrier density of sample 1 after mesa definition [configuration (ii)]. Surprisingly, the Hall coefficient changed sign again, *from n-type back to p-type*. Nevertheless, the activation energy remained the same as before, and the carrier density decreased by almost two orders of magnitude. Since the sign reversal of the Hall coefficient was observed only after RIE process [for the case with no mesa (i)] it is important to study whether the RIE treatment of a B doped diamond sample leads to a change in measured carrier type, i.e., to investigate the result of RIE treatment on a well defined mesa of a B doped diamond before and after oxygen plasma. Figure 2 depicts Arrhenius plot of the carrier density for another boron doped diamond (sample 2) before and after mesa definition and following RIE treatment of the mesa. As discussed above, the as grown sample (sample 2) measured in configuration (i) exhibits p-type (squares) with two activation energies and quite high carrier density at high temperature (exceeding the B concentration according to SIMS). After mesa definition the carrier type remains p-type, however the hole density decreases by one order of magnitude and a single activation energy of E_a=0.33 eV is observed (circles). Sample 2 was exposed to O_2 RIE with the same parameters as sample 1 and Hall measurements were performed. Figure 2 presents the carrier density before (circles) and after (triangles) RIE with mesa (taking into account the thickness loss due to the RIE). The mobilities measured at different temperatures for these cases are shown in Fig. 3. The mobility of the as grown sample (sample 2) measured with no mesa is lower than that measured with the mesa structure by about a factor of 5. Furthermore, there are no significant differences in the measured mobilities for the mesa case due to the RIE treatment. Hence, it is clear that there is *no influence of the RIE on the electrical properties of the top B doped diamond*. This result

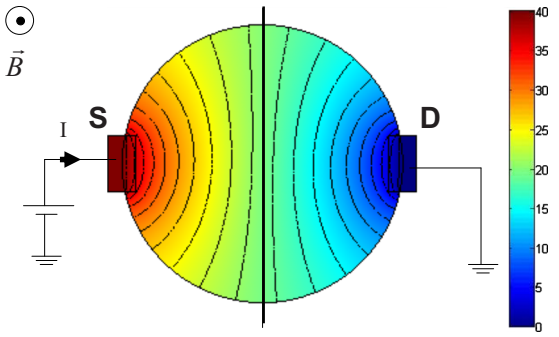

FIG. 4. (Color online) Finite element simulation of equipotential lines for a boron doped sample into which current is injected from left to right, placed in a perpendicular magnetic field.

implies that the *sign reversal of the Hall coefficient after RIE treatment of non mesa sample is an artifact of the measurement*. It can be attributed to the current flowing in the more conductive side facets of the diamond samples giving rise to the erroneous observed carrier sign reversal (further discussed below) and to the higher carrier concentration. We estimate, based on the dimensions of the sample ($3\times3\times1$ mm^3) and the different B concentrations measured by SIMS ($B^S \approx 10\times B^T$), that as much as 25 times more current may flow, without a mesa, through the thick highly doped side facets of the sample, in agreement with the experimental data. The erroneous extracted mobility for the as grown sample is a consequence of the incorrect determination of the carrier density. We believe that the oxygen treatment through the RIE has modified the current distribution along the non-mesa samples and as a result sign reversal of the Hall coefficient was observed.

To explain the present results we have applied the COMSOL simulation program[11] with the ac/dc module that supports quasistatic electromagnetic calculations to simulate the expected current trajectories, equipotential lines, and Hall voltages for different measurement configurations. First, in order to verify that indeed the simulation is capable of predicting the Hall effect we have simulated the equipotential lines for a boron doped sample (circle of 1.3 mm in diameter) into which current is injected from left (source) to right (drain), placed in a perpendicular magnetic field (out of the page). The result is shown in Fig. 4. The asymmetry in the lines with respect to the diagonal line is clearly visible-it represents the Hall voltage. For zero magnetic field one obtains zero Hall voltage as expected.

Three different contact configurations to a B doped diamond lamella of constant thickness of 0.75 μm, however with different conductivity profiles, placed in a uniform magnetic field of 0.8 T perpendicular to the surface were simulated. The central part of the doped layer was always with a constant conductivity of $\sigma_0=0.165$ S/m at room temperature (RT), typical for a doped diamond with a boron concentration of 10^{18} cm^{-3}. The changes in conductivity in the three modeled configurations are assumed to be either due to changes in carrier density or due to changes in carrier mobility. The sizes of the modeled samples (I, II, and III), their carrier concentration and mobility distributions as well as the contact configurations are shown in Fig. 5 and discussed below. The geometries that were used in the simulations correspond to the ones we have used in the experiments. In all cases the current was flowing from contact S to contact D and a voltage of 40 V was applied between these contacts. Figures 5(a) and 5(b) depict the assumed carrier concentration and carrier mobility profiles used in the simulations. The simulated results of the Hall voltages along the dashed lines in Fig. 5(a) located on the symmetry axis of the sample for different contact locations r (expressed as a fraction of the sample size a) are shown in Figs. 6 and 7 for the different carrier concentration and mobility distributions, respectively, given in Fig. 5. The nonmonotonic behavior of some of the curves indicates a *sign reversal in the measured Hall effect* that depends on the r/a contact location, i.e., a possible reversal of deduced carrier type.

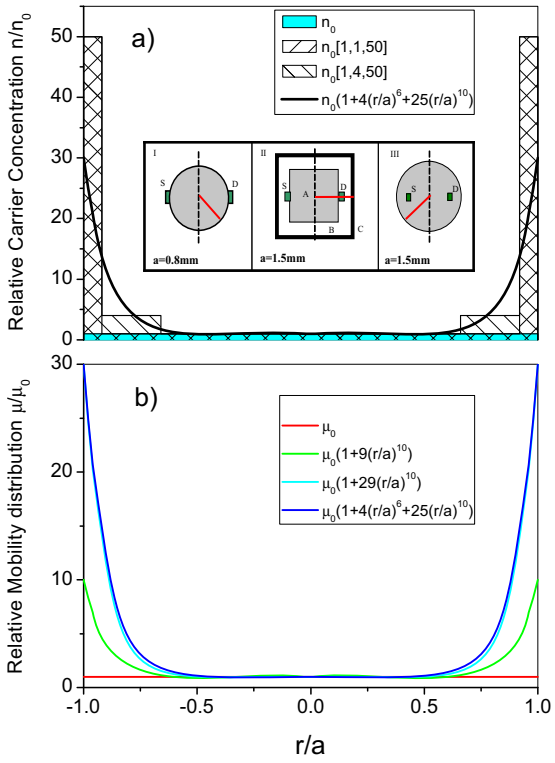

FIG. 5. (Color online) Model shape, carrier, and mobility distributions taken for the electromagnetic simulation. The current is flowing between source (s) and drain (d) contacts, and Hall voltage is simulated along the dashed line located on the symmetry axis of the sample. Figure 5(a): carrier density inhomogeneity distribution. Relative carrier distribution for three different models are shown: (I) mesa structure with homogenous carrier distribution ($n=n_0$), and radius $a=0.8$ mm (mark in red), (II) square shape sample (3×3 mm^2) with three different areas of carrier concentrations, $n=[n_A,n_B,n_C]$, ($n=n_0[1,1,50]$ or $n=n_0[1,4,50]$) in regions A, B, and C, respectively, (see text), (III) round shape sample with graded carrier density $\{n=n_0[1+4(r/a)^6+25(r/a)^{10}]\}$ where $a=1.5$ mm, and n_0 is the RT carrier density for boron doping of 2×10^{18} cm^{-3}. Figure 5(b): mobility inhomogeneity distribution for configuration (III) in Fig. 5(a). Relative mobility distribution for four different mobility variations are shown: (i) round shape sample with homogenous RT mobility for boron doping of 2×10^{18} cm^{-3} with $\mu_0=400$ cm^2/V sec. (ii) Round shape sample with graded mobility of the form $\mu(r)=\mu_0(1+9(r/a)^{10})$. (iii) Round shape sample with graded mobility of the form $\mu(r)=\mu_0(1+29(r/a)^{10})$. (iv) Round shape sample with graded mobility of the form $\mu(r)=\mu_0(1+4(r/a)^6+25(r/a)^{10})$.

The following should be noted:

(i) sample I in Fig. 5(a) represents a homogenously doped circular mesa structure of 1.6 mm diameter.

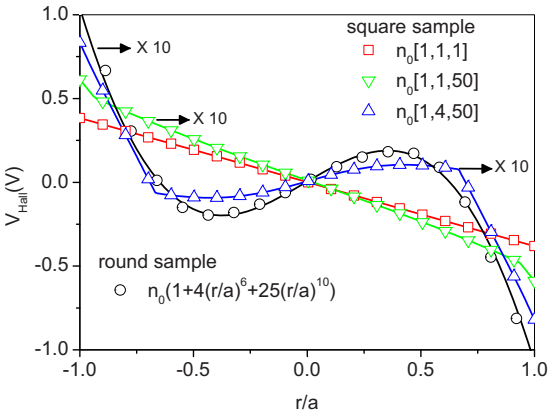

FIG. 6. (Color online) Simulated results for Hall voltage for inhomogeneous density distribution along the dashed line in Fig. 5. The homogeneous mesa sample (square) as well as the inhomogeneous square sample (down triangular) with $n=n_0[1,1,50]$ show no sign reversal for the Hall voltage. For stronger inhomogeneity of the type $n=n_0[1,4,50]$ (up triangular) or $n=n_0(1+4(r/a)^6+25(r/a)^{10})$ (circle) indeed sign reversal of the Hall voltage is predicted for interior Hall contacts.

The results of the simulations show a monotonic linear dependence of the Hall voltage along the dashed line, yielding the same experimental sign for the Hall voltage for any position of the contacts. This holds for both constant carrier concentration (n_0) and constant mobility (μ_0) as expected (open squares in Figs. 6 and 7).

(ii) Sample II in Fig. 5(a) represents an inhomogeneous conductivity distribution over a conductive square (3×3 mm^2) taken for the simulation. It is composed of the central part with a conductivity of σ_0 (area A of 1.8×1.8 mm^2) surrounded by a frame of 0.5 mm width (area B) with a conductivity of $\alpha\sigma_0$ (α is a constant to be determined). A third area C of 100 μm width surrounds area B with a conductivity of $50\sigma_0$. The simulations of this configuration (Fig. 6) show that if the current contacts are within an area of identical conductivity as the interior one ($\alpha=1$), there is no sign reversal even in the case where the conductivity of the edges (area C) is 50 times higher than that of area A (down triangular). However, the calculated carrier concentration, based on Hall voltage between two interior contacts, is almost ten times higher than the actual carrier density of area A since some fraction of the current is flowing at the exterior parts. This is in agreement with the carrier concentration differences observed without and with mesa structures in Figs. 1 and 2. If the region between the source (S) and drain (D) contacts and the surroundings facets is conductive enough ($\alpha=4$), a clear sign reversal is obtained (up triangular).

(iii) Sample III is a round disk of 3 mm in diameter with a radially graded conductivity. Two contacts pads of 200×200 μm^2 were located 500 μm from the sample edge. For inhomogeneous carrier density the conductivity is taken to be $\sigma(r)=\sigma_0[1+m(r/a)^l+k(r/a)^n]$ where $r=a$ at the edge of the sample. For example, for $n=10$, $m=0$, and $k=29$ a sample with a very uniform conductivity throughout its area except for a narrow area at the edge of the sample where the conductivity reaches higher values (up to $30\sigma_0$) is obtained. This enables a substantial fraction of the current to flow "behind" the contacts resulting in a Hall sign reversal. For almost the same conductivity distribution but with $m=4$ and $l=6$ the sign reversal is even more significant as is seen in Fig. 6 (circle). This arises from conductivity increase in the intermediate part between the center and the edges of the round sample which facilitates current escaping behind the source and drain contacts.

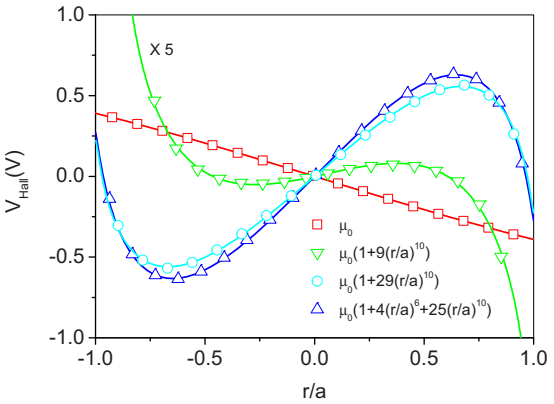

FIG. 7. (Color online) Simulated results for Hall voltage for inhomogeneous mobility distribution along the dashed line in Fig. 5. For inhomogeneous graded distribution (down triangular) sign reversal is observed. For stronger inhomogeneities (circle and up triangular) the sign reversal is an order of magnitude larger than for the carrier density inhomogeneities for similar conductivity inhomogeneities.

The conductivity increment at the surrounding part of the sample may originate from mobility increase as well. When the mobility behaves as $\mu(r)=\mu_0[1+9(r/a)^{10}]$ [Fig. 5(b)] where $\mu_0=400$ cm^2/V sec, sign reversal is indeed found in the simulations if the contacts are not placed at the very edges of the sample (Fig. 7, down triangular). For larger inhomogeneities of type $\mu(r)=\mu_0[1+29(r/a)^{10}]$ or $\mu(r)=\mu_0[1+4(r/a)^6+25(r/a)^{10}]$ the sigh reversal of the Hall voltage increases (circle and up triangular, respectively). Moreover, this sign reversal is almost an order of magnitude more significant for identical contact locations for changes in the mobilities than for changes in carrier densities with similar inhomogeneities of the conductivity. However the case of conductivity inhomogeneity due to changes in mobility is unlikely since nonrealistic mobilities (at least an order of magnitude larger than for typical B-doped diamonds) at the sample sides are required to simulate the experimental results.

Recently, sign reversal of carrier type was measured experimentally in a ZnO thin film.[12] The origin for the wrong sign was attributed to inhomogeneity of carrier concentrations over the entire sample and to the positioning of the electrical contacts located in that case at the interior of the sample. Our measurements are in agreement with their conclusions as well. An attempt to reproduce the influence of the conductive surroundings on the results of the Hall measurements was done in Ref. 13 utilize a finite element simulation.

In their simulation only for nonuniform carrier concentration (and nonmobility) sign reversal in the Hall coefficient was obtained. However, in our simulations an even more pronounce sign reversal was found for samples with non uniform mobility distribution. Taking into account that Hall voltage is proportional to current/density one may anticipate stronger influence for nonuniform mobility than for carrier distribution.

IV. CONCLUSION

Experimental and theoretical results of Hall and conductivity measurements of boron doped diamonds in VdP configuration were presented. We have shown experimentally that a false carrier type can be deduced from Hall effect measurements if the contacts are placed on the sample in such positions that some current may flow outside of the area enclosed by the contacts. Measurements on mesa structured samples, for which such a "sneaking through" behind the contacts is impossible, yield accurate carrier type, density, and mobility results. RIE by oxygen plasma has no effect on the electrical properties of boron doped structures, once properly measured using a mesa to electrically isolate the measured regions. Finite element quasielectrostatic simulations on samples with different carrier concentrations or mobilities and different contact locations confirm the possibility of obtaining erroneous results from VdP measurements when the measured doped area is not restricted (i.e., with no mesa). For samples with nonhomogenous doping concentrations, i.e., with surrounding facets that conduct much better than the interior part measured with no mesa, show both experimentally and theoretically, that erroneous conclusion on the effect of RIE of oxygen plasma on the B doped diamond, and possibly on other doped diamond samples can be obtained.

On the basis of these results, one should carefully reconsider the sign reversal of the Hall coefficient on hydrogen plasma exposed B doped diamond samples (in which HBH complexes were formed, as deduced by SIMS) for which in some cases n-type conduction was deduced from Hall effect measurements.[14] In some of these samples non homogenous boron doped areas exist due to the presence of growth sectors in the substrate diamond as analyzed from cathodoluminescence experiments yielding different doping efficiencies.[6] Furthermore, some B doping on the side facets of the samples may have occurred. As the samples following expose to a hydrogen (deuterium) plasma were measured in VdP configuration without mesa structures, some wrong conclusions may have been obtained due to the above mentioned points. We believe that measuring B doped samples following exposure to a hydrogen plasma after mesa definition may clarify the situation regarding n-type doping of diamond by the formation of B–H complexes.

ACKNOWLEDGMENTS

This work was partially supported by The Israeli Science Foundation under Grant No. 686/06 and the Russell Berrie Nanotechnology Institute.

[1] S. Koizumi, K. Watanabe, F. Hasegawa, and H. Kanda, Science **292**, 1899 (2001).
[2] E. Kohn, M. Adamschik, P. Schmid, A. Denisenko, A. Aleksov, and W. Ebert, J. Phys. D: Appl. Phys. **34**, R77 (2001).
[3] M. Nesladek, Semicond. Sci. Technol. **20**, R19 (2005).
[4] R. Kalish, C. Saguy, C. Cytermann, J. Chevallier, Z. Teukam, F. Jomard, T. Kociniewski, D. Ballutaud, J. E. Butler, C. Baron, and A. Deneuville, J. Appl. Phys. **96**, 7060 (2004).
[5] M. A. Pinault, J. Barjon, T. Kociniewski, F. Jomard, and J. Chevallier, Physica B **401**, 51 (2007).
[6] N. Habka, M. A. Pinault, C. Mer, F. Jomard, J. Barjon, M. Nesladek, and P. Bergonzo, Phys. Status Solidi A **205**, 2169 (2008).
[7] Z. Teukam, J. Chevallier, C. Saguy, R. Kalish, D. Ballutaud, M. Barbe, F. Jomard, A. Tromson-Carli, C. Cytermann, J. E. Butler, M. Bernard, C. Baron, and A. Deneuville, Nature Mater. **2**, 482 (2003).
[8] H. Okushi, Diamond Relat. Mater. **10**, 281 (2001).
[9] Dry etch was done at 50 mTorr with 30SCCM flow of oxygen and 110 W power. The NiCr mask was removed by soaking the sample in 1:1:3 solution of percloric acid, sulfuric acid, and fuming nitric acid for 15 min at 120 °C.
[10] J. P. Lagrange, A. Deneuville, and E. Gheeraert, Carbon **37**, 807 (1999).
[11] www.comsol.com/products/multiphysics/education/tutorials
[12] T. Ohgaki, N. Ohashi, S. Sugimura, H. Ryoken, I. Sakaguchi, Y. Adachi, and H. Haneda, J. Mater. Res. **23**, 2293 (2008).
[13] O. Bierwagen, T. Ive, C. G. Van de Walle, and J. S. Speck, Appl. Phys. Lett. **93**, 242108 (2008).
[14] C. Saguy, R. Kalish, J. Chevallier, F. Jornard, C. Cytermann, B. Philosoph, T. Kociniewski, D. Ballutaud, C. Baron, and A. Deneuville, Diamond Relat. Mater. **16**, 1459 (2007).